Research Square

Preprints are preliminary reports that have not undergone peer review.
They should not be considered conclusive, used to inform clinical practice,
or referenced by the media as validated information.

Effect of NiO-BiVO4 Composition Variation on Elemental Distribution and Surface Morphology Based on SEM-EDX Characterization

Achmad Walid

achmad.walid@polinema.ac.id

Malang State Polytechnic

Nafila Faustina Yulia Salsabila

Institut Teknologi Sepuluh Nopember

Research Article

Keywords: NiO, BV, BiVO4, SEM-EDX, metal oxide composite, elemental distribution

Posted Date: June 23rd, 2026

DOI: https://doi.org/10.21203/rs.3.rs-10102686/v1

License: This work is licensed under a Creative Commons Attribution 4.0 International License.
Read Full License

Additional Declarations: No competing interests reported.

Effect of NiO-BiVO4 Composition Variation on Elemental Distribution and Surface Morphology Based on SEM-EDX Characterization

Achmad Walid[1]*, Nafila Faustina Yulia Salsabila[2]

[1]*Department of Mechanical Engineering, Malang State Polytehnic, Soekarno Hatta Avenue No. 9, Jatimulyo, Lowokwaru District, Malang City, East Java, 65141, Indonesia*

[2]*Department of Materials and Metallurgical Engineering, Faculty of Industrial Technology and Systems Engineering, Institut Teknologi Sepuluh Nopember, Jl. Arif Rahman Hakim, Kampus ITS Keputih-Sukolilo, Surabaya 60111, Indonesia*

*Corresponding author: achmad.walid@polinema.ac.id

Abstract

This study investigates the effect of NiO-BiVO4 (NiO-BV) composition variation on elemental distribution and surface morphology using scanning electron microscopy-energy dispersive X-ray spectroscopy (SEM-EDX). Six composition variations were evaluated, namely 0 NiO-100 BV, 20 NiO-80 BV, 40 NiO-60 BV, 60 NiO-40 BV, 80 NiO-20 BV, and 100 NiO-0 BV. The EDX results showed that the 0 NiO-100 BV sample was dominated by Bi, V, and O, whereas the 100 NiO-0 BV sample was dominated by Ni and O. Increasing the NiO fraction generally increased the Ni content, while Bi and V tended to decrease as the BV fraction was reduced. The intermediate compositions exhibited non-linear compositional behavior, which can be attributed to surface heterogeneity, particle agglomeration, and the localized nature of EDX measurements. Representative SEM-EDX images of each variation further confirmed the transition from a BV-rich surface to a NiO-rich surface. These findings indicate that the NiO/BV ratio affects both elemental distribution and surface morphology. Further characterization using XRD, FTIR, UV-Vis DRS, and photocatalytic or photoelectrochemical tests is recommended to confirm phase structure, functional groups, optical properties, and material performance.

Keywords: NiO, BV, BiVO4, SEM-EDX, metal oxide composite, elemental distribution.

1. Introduction

Metal oxide materials have been widely developed as functional materials because of their chemical stability, tunable composition, and potential applications in photocatalysis, photoelectrochemistry, sensors, and wastewater treatment. According to Bai et al. (2025), BiVO4-based heterojunctions are highly attractive for energy and environmental applications. Zhang et al. (2025) specifically highlighted BiVO4 as a visible-light-responsive photocatalyst for degradation processes, while Nguyen et al. (2025) and Navarrete-Cevallos et al. (2025) emphasized its relevance for photoelectrochemical water splitting and water treatment. In broader reviews, Guan et al. (2024), Kamble et al. (2023), and Sindhu et al. (2026) further explained that the performance of BiVO4 can be improved through synthesis control, morphology engineering, doping, heterojunction formation, and cocatalyst modification.

Despite its potential, BiVO4 still suffers from charge recombination and limited charge-transfer efficiency. Heckel et al. (2024) emphasized that surface chemistry and morphology strongly affect the activity of BiVO4-based materials, and Tachikawa et al. (2016) showed that crystal-facet-dependent charge dynamics can directly influence surface reactivity. In photoelectrochemical systems, Salih et al. (2024), Cheng et al. (2025), and Wan et al. (2023) demonstrated that cocatalyst design and surface modification improve water-oxidation performance. Likewise, Long et al. (2024), Mohan et al. (2025), and Chen et al. (2025) reported that heterojunction engineering can enhance interfacial charge transport and visible-light photocatalytic behavior.

Nickel oxide (NiO) is a transition metal oxide frequently used in photocatalytic and composite oxide systems. NiO can function as an active material, support material, or cocatalyst in heterostructured systems. Wang et al. (2022) reported that incorporating NiO into BiVO4 improved photoelectrochemical performance by promoting charge transfer and providing additional active surface sites. Related Ni-containing photocatalysts have also been reported by Minisha et al. (2024), Pavithra et al. (2023), Gomaa et al. (2024), and Yasmeen et al. (2024), who showed that compositional tuning and binary-oxide coupling can substantially alter degradation efficiency and surface reactivity. In a NiO-BV composite system, changing the ratio of NiO and BV is therefore expected to influence the surface concentrations of Ni, Bi, V, and O.

SEM-EDX characterization is an important initial step to evaluate composite formation. SEM provides information about morphology, texture, and surface contrast, whereas EDX identifies the detected elements and estimates their relative concentrations in terms of weight percentage (wt%) and atomic percentage (at%). Wannakan et al. (2023), Sisay et al. (2023), Cai et al. (2015), and Lecki et al. (2024) used SEM-EDX-related characterization to confirm heterojunction formation and compositional distribution in BiVO4-based systems. Reyes-Vallejo et al. (2025), Le-Duy et al. (2023), and Fu et al. (2024) further demonstrated that SEM combined with elemental analysis is useful for identifying the main elements and possible minor or impurity elements in advanced BiVO4-containing composites.

This study aims to evaluate the effect of NiO-BV composition variation on elemental distribution and surface morphology. The main focus is the change in Ni, Bi, V, and O contents in six composition variations ranging from 0 NiO-100 BV to 100 NiO-0 BV.

2. Materials and Methods

This study used SEM-EDX characterization data from six NiO-BV composite samples with composition variations of 0 NiO-100 BV, 20 NiO-80 BV, 40 NiO-60 BV, 60 NiO-40 BV, 80 NiO-20 BV, and 100 NiO-0 BV. Each variation was analyzed at several EDX measurement points to obtain elemental composition data in weight percent (wt%) and atomic percent (at%).

SEM analysis was used to observe surface morphology and surface contrast at the micrometer scale. The SEM images were evaluated qualitatively to identify differences in texture, contrast, and indications of surface heterogeneity among the composition variations. Such an approach is consistent with BiVO4-based photocatalytic composite studies. For example, Haryadinaru et al. (2025) and Riapanitra et al. (2025) used SEM to discuss morphology in BiVO4/g-C3N4 composites, while Sisay et al. (2022) employed similar morphological evaluation in BiVO4-containing hybrid membranes. Comparable SEM-based interpretations were also reported by Reyes-Vallejo et al. (2025), Pavithra et al. (2023), and Minisha et al. (2024) in oxide photocatalyst systems.

EDX analysis was used to identify the elements detected on the sample surfaces. The main elements evaluated in this study were Ni, Bi, V, and O, while minor elements such as C, Y, Tc, Al, Si, and Ca were treated as secondary elements that may originate from preparation, contamination, substrate contribution, or local variation in the analyzed area. In oxide composite studies, EDX is commonly used to confirm constituent elements and estimate local compositional distribution. Trinh et al. (2021), Orimolade et al. (2020), and Haq et al. (2022) used EDX to verify elemental presence in composite photocatalysts, whereas Le-Duy et al. (2023) and Fu et al. (2024) showed that combining elemental analysis with surface characterization is especially important for interpreting interfacial structure in BiVO4-based materials.

The average wt% and at% values were calculated from four EDX measurement points for each composition. As shown in Table 1, average values and standard deviations were then used to compare the compositional trend of Ni, Bi, V, and O as the nominal NiO fraction increased and the BV fraction decreased.

Table 1. Average elemental composition of the main elements based on EDX data

Sample composition	O (wt%)	Bi (wt%)	V (wt%)	Ni (wt%)	O (at%)	Bi (at%)	V (at%)	Ni (at%)
0 NiO-100 BV	10.20	64.81	16.68	0.00	40.78	19.88	20.98	0.00
20 NiO-80 BV	10.38	47.23	11.68	26.12	38.77	13.75	13.95	26.12
40 NiO-60 BV	12.58	25.04	6.05	53.44	38.79	5.91	5.86	44.93
60 NiO-40 BV	14.48	28.14	6.52	45.16	42.58	6.37	6.06	36.21
80 NiO-20 BV	14.50	25.62	6.51	48.04	42.13	5.74	5.97	38.02
100 NiO-0 BV	12.33	0.00	0.00	87.67	34.00	0.00	0.00	66.00

Note: Values represent the average of four EDX measurement points for each sample composition.

3. Results and Discussion

3.1 Elemental Composition of the 0 NiO-100 BV Sample

The 0 NiO-100 BV sample represents the BV-rich composition. The average Bi content reached 64.81 wt%, V was 16.68 wt%, and O was 10.20 wt%, while Ni was not detected. This result confirms that the initial sample was dominated by the constituent elements of BV. The SEM image showed heterogeneous dark-bright contrast, which may indicate local differences in composition or surface texture. Tachikawa et al. (2016) showed that crystal facets and local surface structure in BiVO4 can influence charge dynamics, and Heckel et al. (2024) also emphasized that morphology-sensitive behavior is a key characteristic of BiVO4-based active materials.

3.2 Elemental Composition of the 20 NiO-80 BV Sample

In the 20 NiO-80 BV sample, Ni was clearly detected with an average value of 26.12 wt%. Meanwhile, Bi and V decreased to 47.23 wt% and 11.68 wt%, respectively. Compared with the 0 NiO-100 BV sample, the decrease in Bi and V indicates the reduced contribution of the BV component, while the appearance of Ni confirms the incorporation of the NiO component into the material system. This change supports the formation of a NiO-BV composite. Wang et al. (2022) reported that NiO modification of BiVO4 can form BiVO4/NiO composites with improved photoelectrochemical performance through enhanced charge transfer.

3.3 Elemental Composition of the 40 NiO-60 BV Sample

The 40 NiO-60 BV sample showed a substantial increase in Ni content, reaching an average of 53.44 wt%. At the same time, Bi decreased to 25.04 wt% and V to 6.05 wt%. This result demonstrates that increasing the NiO fraction strongly affects the surface elemental composition. The O content also increased to 12.58 wt%, which may be related to the oxide nature of both NiO and BV. Cai et al. (2015) and Wannakan et al. (2023) showed that changes in precursor ratio and heterojunction composition can modify surface elemental distribution, particle contact, and the availability of active interfacial regions.

3.4 Elemental Composition of the 60 NiO-40 BV Sample

For the 60 NiO-40 BV sample, the average Ni, Bi, V, and O contents were 45.16 wt%, 28.14 wt%, 6.52 wt%, and 14.48 wt%, respectively. Although the nominal NiO fraction was higher than that of the 40 NiO-60 BV sample, the detected Ni content was lower. This indicates that the elemental distribution on the surface does not always follow the nominal ratio linearly. Such non-linearity may be caused by surface heterogeneity, particle agglomeration, differences in EDX measurement areas, or the dominance of certain local phases in the analyzed region. Sisay et al. (2023) and Trinh et al. (2021) likewise noted that composite materials often show local compositional variability because EDX represents surface information from limited measurement areas rather than the entire bulk composition.

3.5 Elemental Composition of the 80 NiO-20 BV Sample

In the 80 NiO-20 BV sample, the average Ni content was 48.04 wt%, while Bi and V were 25.62 wt% and 6.51 wt%, respectively. The O content was 14.50 wt%, relatively higher than that of the BV-rich samples. The presence of considerable Bi and V contents suggests that BV-rich areas remained on the surface or that the composite was not fully homogeneous. Bai et al. (2025) explained that interfacial contact is critical in BiVO4-based heterojunctions, Lecki et al. (2024) discussed the role of phase coupling in Z-scheme systems, and Orimolade et al. (2020) showed that local elemental distribution can strongly affect charge transfer and functional performance.

3.6 Elemental Composition of the 100 NiO-0 BV Sample

The 100 NiO-0 BV sample exhibited the simplest elemental composition, with Ni at 87.67 wt% and O at 12.33 wt%. Bi and V were not detected. This result agrees with the nominal composition, which contains only NiO. This also supports the validity of the dataset because the NiO-rich end member showed clear Ni-O dominance. Khairnar and Shrivastava (2019),

Khan et al. (2022), Shubha et al. (2023), and Barzinjy et al. (2020) all reported that NiO and NiO-based materials can function as photocatalysts for dye degradation, so this composition is relevant as a NiO-rich reference in the present series.

3.7 General Trend and Material Implications

Overall, increasing the NiO fraction led to the appearance and increase of Ni in the composite system, while decreasing the BV fraction caused Bi and V to decrease. The 0 NiO-100 BV sample was dominated by Bi-V-O, whereas the 100 NiO-0 BV sample was dominated by Ni-O. Intermediate samples contained Ni, Bi, V, and O simultaneously, indicating the formation of NiO-BV composite systems. Iqbal et al. (2025) showed that precursor-support interactions can alter the apparent activity of BiVO4 composites, while Long et al. (2024) and Chen et al. (2025) demonstrated that phase coupling strongly influences interfacial contact and visible-light photocatalytic behavior.

However, the trend was not fully linear. The Ni content in the 40 NiO-60 BV sample was higher than that in the 60 NiO-40 BV and 80 NiO-20 BV samples. This may be associated with uneven particle distribution, surface heterogeneity, or differences in the selected EDX points. Therefore, SEM-EDX results should be interpreted as indications of local surface composition. Zhang et al. (2025), Nguyen et al. (2025), Navarrete-Cevallos et al. (2025), and Cheng et al. (2025) all suggested that additional characterization such as XRD, FTIR, UV-Vis DRS, and photoelectrochemical testing is necessary to verify phase structure and functional performance. Wan et al. (2023) and Mohan et al. (2025) similarly discussed how local morphology and cocatalyst distribution can influence the apparent charge-transfer response of BiVO4-based systems.

From an application perspective, the combination of NiO and BV is promising because both components are relevant in photocatalytic material development. Hariani et al. (2022), Haq et al. (2022), Khairnar and Shrivastava (2019), and Khan et al. (2022) showed that NiO-containing materials can degrade methyl orange, methylene blue, rhodamine B, and Orange II. For BiVO4-based systems, Wannakan et al. (2023), Sisay et al. (2022), Sisay et al. (2023), and Zhao et al. (2019) reported applications in pollutant degradation, wastewater treatment, and photoelectrochemical processes. In addition, Minisha et al. (2024), Gomaa et al. (2024), and Yasmeen et al. (2024) demonstrated that dopant incorporation, nanofiber morphology, and binary oxide coupling can substantially alter degradation efficiency and surface reactivity. Taken together, these reports indicate that the present SEM-EDX characterization can serve as a basis for further investigation of the photocatalytic activity of NiO-BV composites.

3.8 Graphical Analysis of Elemental Composition

To clarify the EDX trend, the average composition of the main elements was visualized in three graphs. Fig. 1 shows the relationship between nominal NiO composition and average elemental content in wt%, Fig. 2 shows the same relationship in at%, and Fig. 3 presents the shift in elemental dominance using a stacked bar chart. The error bars in Figs. 1 and 2 represent the standard deviation of four EDX measurement points for each sample.

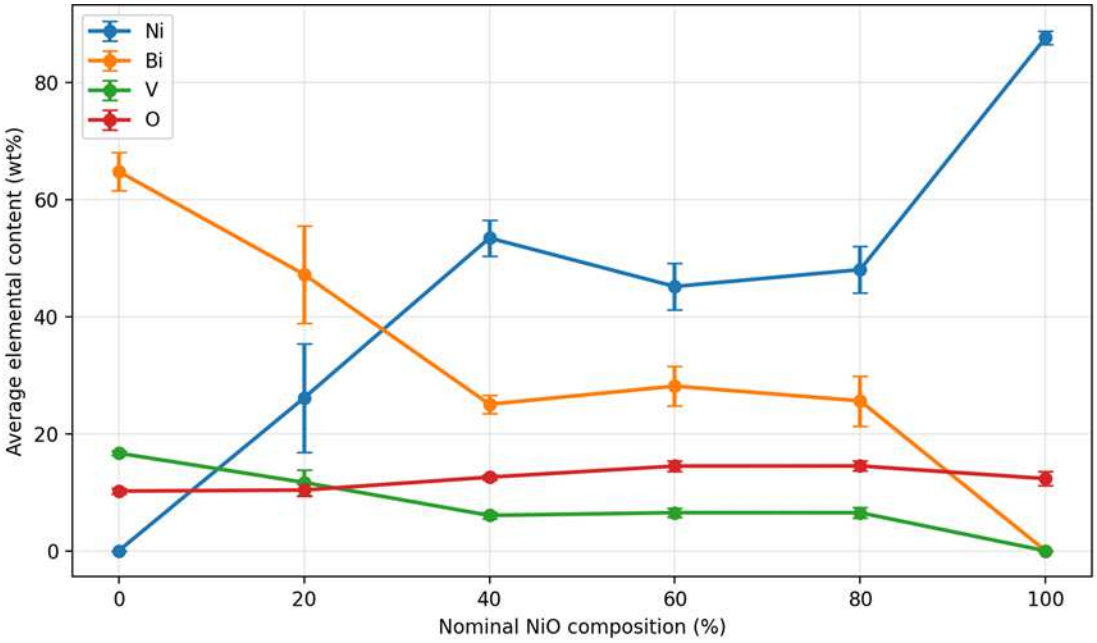


Fig. 1 Trend of average wt% of the main elements as a function of nominal NiO composition

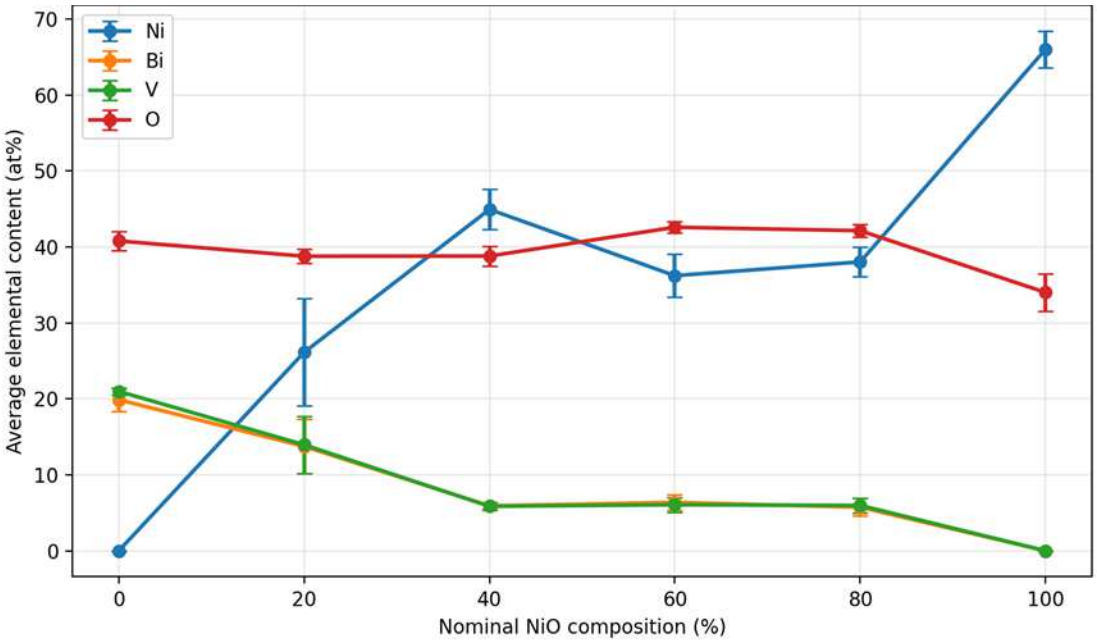


Fig. 2 Trend of average at% of the main elements as a function of nominal NiO composition

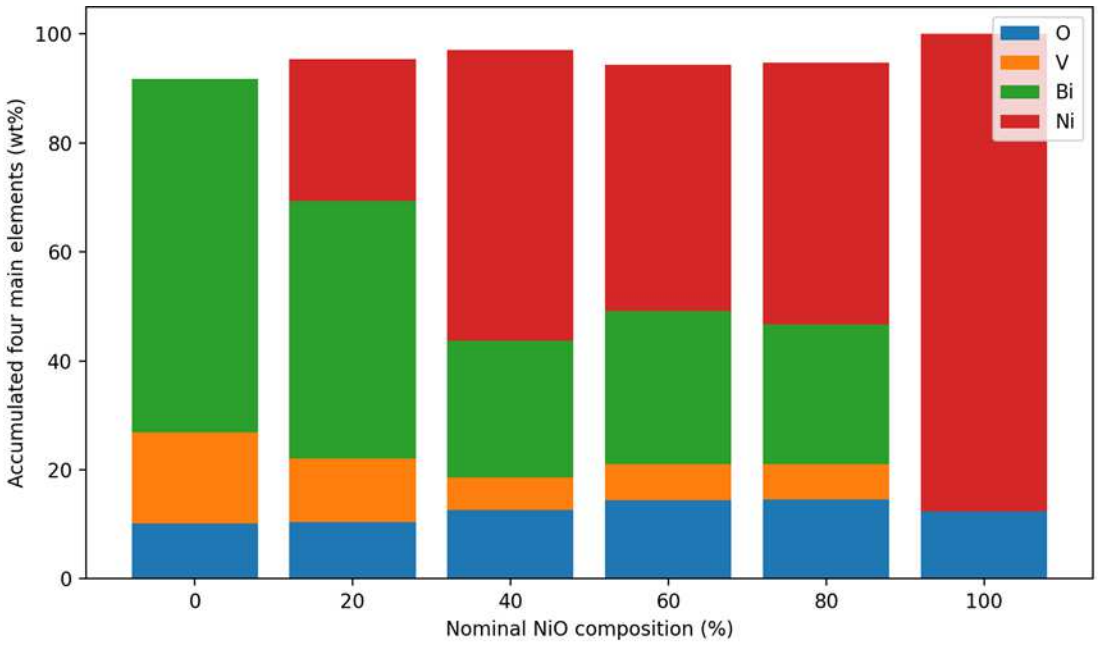


Fig.3 Shift in elemental dominance in the NiO-BV composites based on average wt%

Fig. 1 shows that increasing the nominal NiO composition generally increased the amount of Ni detected on the surface. Ni was not detected in the 0 NiO-100 BV sample, increased to 26.12 wt% in 20 NiO-80 BV, and reached 53.44 wt% in 40 NiO-60 BV. However, Ni decreased slightly in 60 NiO-40 BV and 80 NiO-20 BV, with values of 45.16 wt% and 48.04 wt%, respectively, before reaching 87.67 wt% in 100 NiO-0 BV. This pattern indicates that the relationship between nominal composition and measured composition is not fully linear, particularly in the intermediate compositions.

At the same time, Bi and V showed a clear decreasing trend as the BV fraction was reduced. Bi decreased from 64.81 wt% in 0 NiO-100 BV to 47.23 wt% in 20 NiO-80 BV, then remained around 25-28 wt% in the 40-80 NiO compositions, and finally disappeared in the 100 NiO-0 BV sample. V also decreased from 16.68 wt% to approximately 6.05-6.52 wt% in the intermediate compositions and was not detected in the pure NiO sample. These trends confirm that Bi and V are the main indicators of the BV component in the composite system.

Fig. 2 indicates that the same general pattern remained consistent when the data were expressed in atomic percentage. Oxygen showed relatively stable values in the composite compositions, approximately 38.77-42.58 at%, indicating that oxygen remained an important element in all oxide systems. Ni increased from 0 at% in the sample without NiO to 66.00 at% in the 100 NiO-0 BV sample, whereas Bi and V decreased sharply. In atomic percentage, the dominance of oxygen appears stronger than in weight percentage because oxygen has a much lower atomic mass than Ni, Bi, and V.

Fig. 3 clarifies the transition of material characteristics from a BV-rich composition to a NiO-rich composition. In 0 NiO-100 BV, the four main elements were dominated by Bi-V-O. In the intermediate compositions, Ni, Bi, V, and O were detected simultaneously, strengthening the indication of NiO-BV composite formation. In 100 NiO-0 BV, the main contribution shifted almost entirely to the Ni-O system. This visualization supports the interpretation that changing the precursor ratio gradually shifted the chemical identity of the material from a BV-rich phase toward a NiO-rich phase.

In addition to showing general trends, the graphs also reveal relatively large error bars in some compositions, especially in the 20 NiO-80 BV sample for Ni and Bi. This suggests considerable local variation among EDX measurement points. Therefore, the graphical analysis reinforces the interpretation that EDX results represent local surface composition and are influenced by particle distribution heterogeneity, agglomeration, and possible incomplete homogenization during material preparation.

3.9 SEM-EDX Image Analysis for Each Composition Variation

In addition to numerical and graphical evaluation, the SEM-EDX images of each composition variation were analyzed to relate the local elemental composition to the observed surface morphology. The interpretation was performed qualitatively by considering the dominant EDX peaks, the elemental table attached to each microanalysis report, and the surface contrast in the SEM micrographs. Wannakan et al. (2023), Sisay et al. (2023), and Trinh et al. (2021) showed that SEM-EDX is widely used in metal oxide composite studies because it can simultaneously reveal surface texture and elemental signatures, although the results should be interpreted as local surface information rather than bulk composition. Reyes-Vallejo et al. (2025), Le-Duy et al. (2023), and Fu et al. (2024) further emphasized that combining SEM with EDX, XPS, and complementary phase analysis is essential for correlating local morphology with interfacial chemistry in BiVO4-based and Ni-containing composites.

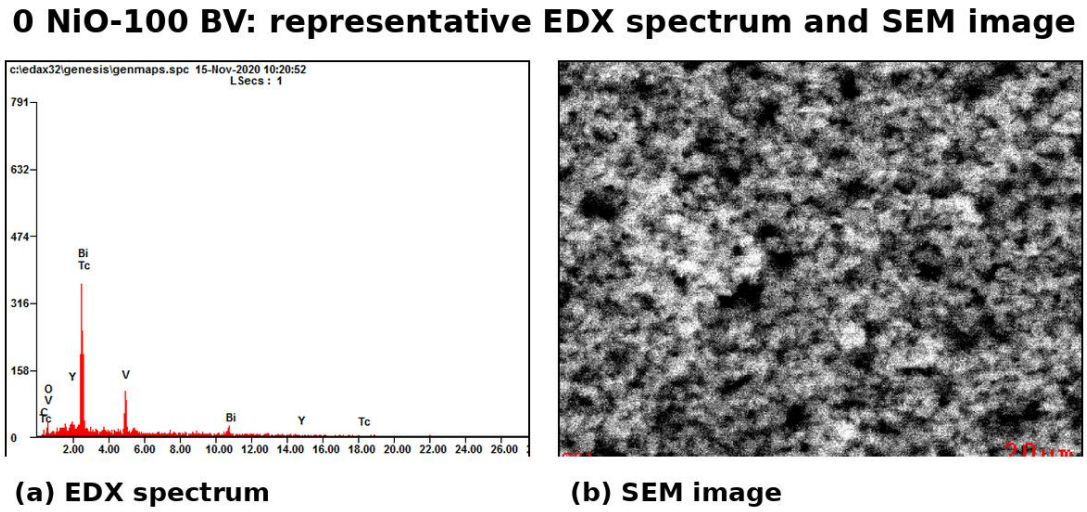


Fig. 4 Representative EDX spectrum and SEM micrograph of the 0 NiO-100 BV sample

In Fig.4, the EDX spectrum exhibited dominant Bi and V peaks together with an O peak, while Ni was absent. This is consistent with the average EDX data, where Bi, V, and O were 64.81 wt%, 16.68 wt%, and 10.20 wt%, respectively. The SEM micrograph showed a relatively heterogeneous surface with dark and bright contrast regions, suggesting local differences in surface texture and elemental distribution. Tachikawa et al. (2016) showed that differences in crystal facets and local surface structure in BiVO4 influence charge dynamics, whereas Heckel et al. (2024) reviewed how morphology-dependent behavior affects the activity of BiVO4-based materials. Therefore, the heterogeneous texture observed in this BV-rich sample is relevant for subsequent functional evaluation.

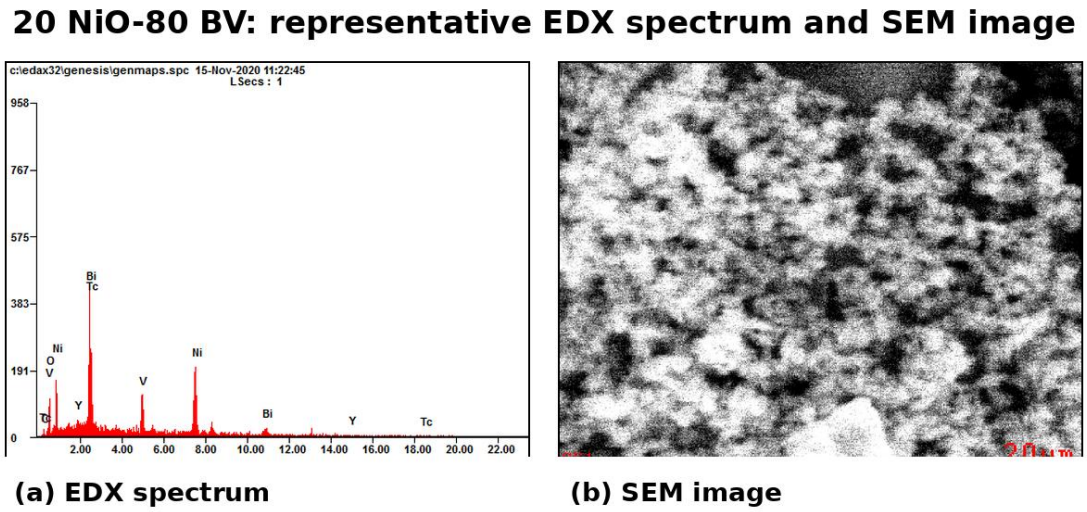


Fig.5 Representative EDX spectrum and SEM micrograph of the 20 NiO-80 BV sample

For the 20 NiO-80 BV variation in Fig.5, the Ni peak began to appear in the EDX spectrum together with Bi, V, and O. The appearance of Ni indicates that the NiO component was introduced into the composite system, while the continued presence of strong Bi and V peaks confirms that the BV-rich character remained dominant. The average Ni content of 26.12 wt% supports the initial incorporation of NiO. The SEM image displayed a fine and non-uniform texture, indicating that the early addition of NiO may have created localized Ni-containing regions on the BV matrix. Wang et al. (2022) reported that NiO-modified $BiVO_4$ composites can improve interfacial charge transfer and photoelectrochemical behavior, highlighting the importance of compositional interaction between NiO and $BiVO_4$/BV phases.

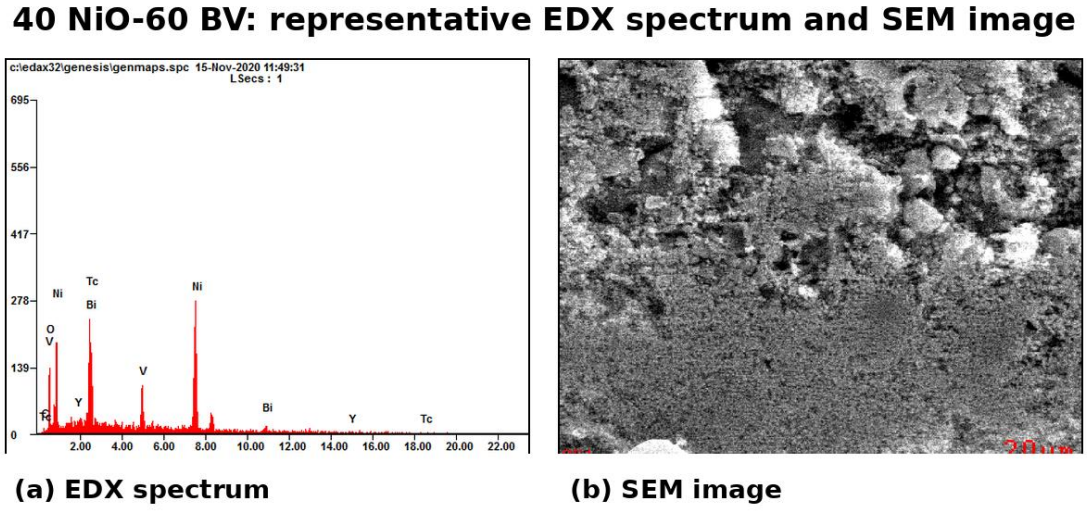


Fig 6. Representative EDX spectrum and SEM micrograph of the 40 NiO-60 BV sample

In Fig. 6, the Ni peak appeared stronger than the Bi and V peaks, matching the average EDX result in which Ni increased to 53.44 wt%, while Bi and V decreased to 25.04 wt% and 6.05 wt%, respectively. The SEM micrograph showed a denser texture with fine particle distribution across the analyzed area. This composition represents a clear transition from a BV-dominant surface toward a NiO-enriched composite surface. Cai et al. (2015) and Wannakan et al. (2023) associated similar compositional changes in oxide heterostructures with modifications in particle contact, surface active sites, and interfacial charge-transfer pathways.

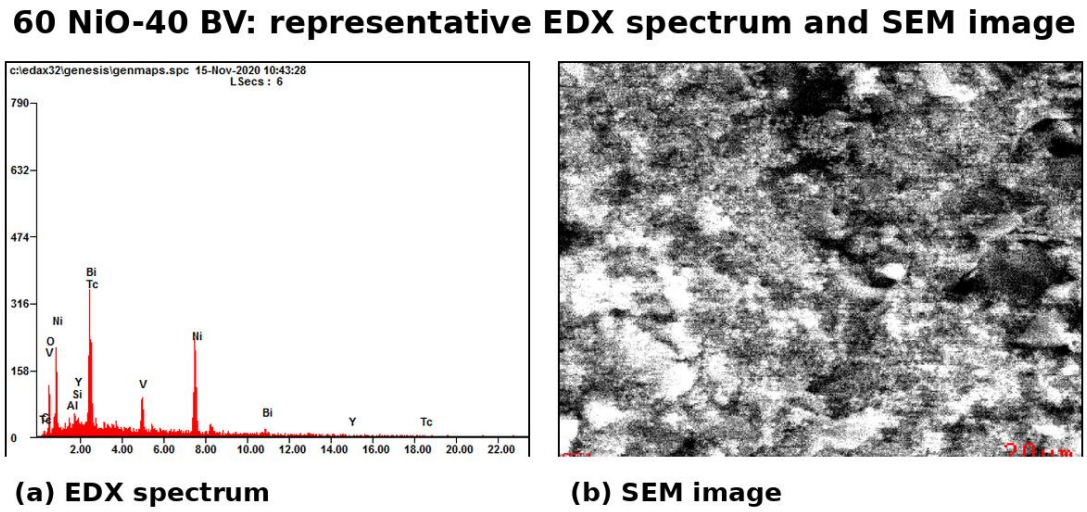


Fig. 7 Representative EDX spectrum and SEM micrograph of the 60 NiO-40 BV sample

In Fig.7, the EDX spectrum still showed Ni together with Bi, V, and O peaks. Although the nominal NiO content was higher than that of the 40 NiO-60 BV sample, the average detected Ni content was lower, namely 45.16 wt%. The SEM image indicated a rougher and more heterogeneous morphology, suggesting that particle agglomeration or uneven distribution may have affected the EDX measurement area. This supports the interpretation that the non-linear trend in the intermediate compositions is related to local surface heterogeneity rather than a simple stoichiometric relationship. Sisay et al. (2023) and Trinh et al. (2021) similarly reported that composite oxide systems often display strong local phase effects because EDX probes only a limited region of the surface.

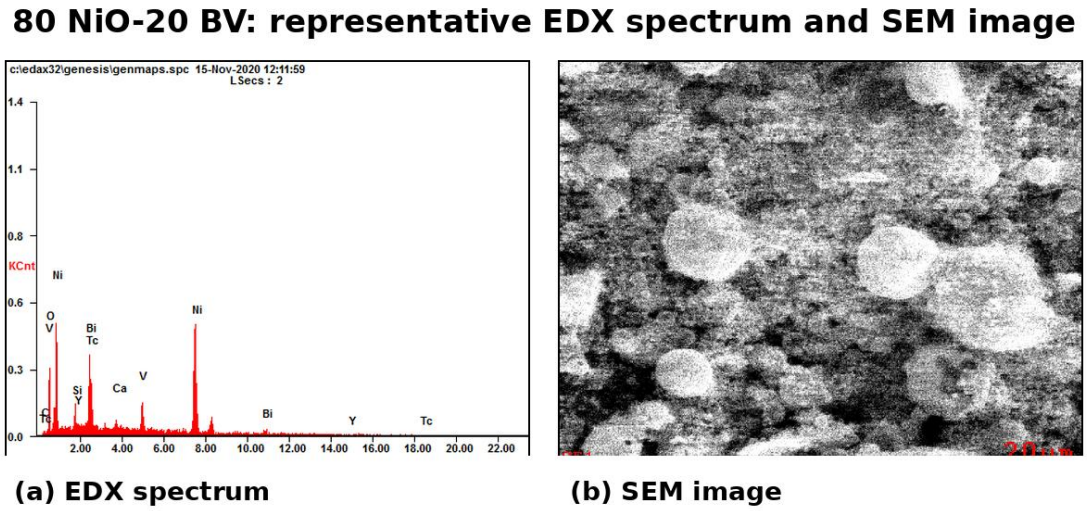


Fig. 8 Representative EDX spectrum and SEM micrograph of the 80 NiO-20 BV sample

For the 80 NiO-20 BV sample in Fig. 8, Ni remained a dominant element, but Bi and V were still detected in the spectrum. The presence of Bi and V at a low nominal BV fraction suggests that BV-rich regions were still present on the analyzed surface or that the mixing process produced non-uniform local distribution. The SEM image showed a granular and contrasted texture, which is consistent with the coexistence of NiO-rich and BV-containing domains. Bai et al. (2025) explained that the spatial distribution of constituent phases is important in BiVO4-based heterojunctions, Lecki et al. (2024) discussed the significance of phase coupling, and Orimolade et al. (2020) demonstrated that interfacial contact can affect charge separation and photocatalytic behavior.

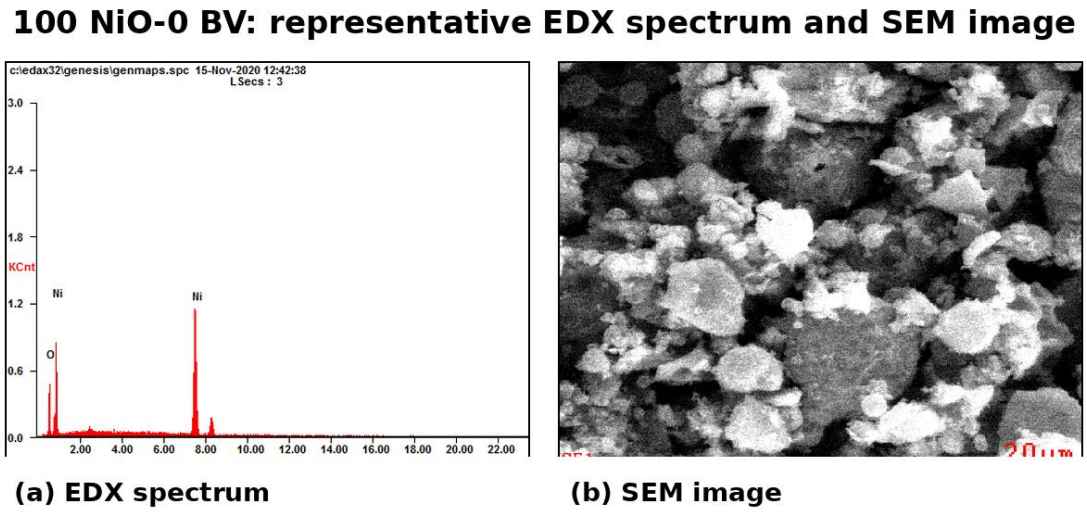


Fig. 9 Representative EDX spectrum and SEM micrograph of the 100 NiO-0 BV sample

In Fig. 9, the EDX spectrum showed only the main elements Ni and O, while Bi and V were not detected. This composition agrees with the characteristics of the NiO end member, with average Ni and O contents of 87.67 wt% and 12.33 wt%, respectively. The SEM micrograph showed a granular surface with relatively strong contrast. The dominance of Ni-O confirms that this sample represents the NiO-rich endpoint of the composition series. Khairnar and Shrivastava (2019), Khan et al. (2022), Shubha et al. (2023), and Barzinjy et al. (2020) all described NiO nanoparticles or NiO-based composites as photocatalytic materials for organic dye degradation, making this composition relevant as a reference material for future performance testing.

Overall, the SEM-EDX image series confirms the compositional transition from a BV-rich material to a NiO-rich material. In the 0 NiO-100 BV sample, the EDX spectrum was dominated by Bi and V; in the intermediate compositions, Ni appeared together with Bi and V; and in the 100 NiO-0 BV sample, the material was dominated by Ni and O. The SEM micrographs also support the graphical analysis by showing heterogeneous and granular surface features in several intermediate compositions. Zhang et al. (2025), Nguyen et al. (2025), Navarrete-Cevallos et al. (2025), and Cheng et al. (2025) all emphasized that additional phase and structural analyses such as XRD, FTIR, UV-Vis DRS, and elemental mapping are needed to confirm phase formation and spatial distribution. Long et al. (2024), Mohan et al. (2025), and Chen et al. (2025) further showed that local domain distribution and interfacial coupling govern the observed response of advanced BiVO4 heterojunctions and surface-engineered composites.

4. Conclusion

SEM-EDX characterization of six NiO-BV composition variations showed that the NiO/BV ratio influenced both surface elemental distribution and morphological characteristics. The tables, graphs, and SEM-EDX images consistently revealed that the 0 NiO-100 BV sample was dominated by Bi, V, and O, whereas the 100 NiO-0 BV sample was dominated by Ni and O. In the mixed compositions, Ni, Bi, V, and O were detected simultaneously, indicating the formation of NiO-BV composite systems. Increasing the NiO fraction generally increased the Ni contribution and reduced the Bi-V contribution, although the intermediate compositions did not follow a fully linear trend. This non-linearity was likely caused by surface heterogeneity, particle agglomeration, and the localized nature of EDX measurements. The SEM-EDX images further supported this interpretation by showing non-uniform surface contrast and granular features across several compositions. Therefore, the elemental and morphological characteristics of NiO-BV composites can be modified through composition ratio adjustment. Further work using XRD, FTIR, UV-Vis DRS, elemental mapping, and photocatalytic or photoelectrochemical testing is recommended to correlate the observed composition with phase structure and functional performance. Guan et al. (2024), Kamble et al. (2023), and Sindhu et al. (2026) likewise emphasized that heterojunction construction, morphology control, and surface engineering remain central strategies for improving BiVO4-based functional materials and related oxide composites.

Acknowledgments

The authors acknowledge the availability of SEM-EDX microanalysis data used as the basis for this manuscript.

Funding Declaration

This research received no specific grant from any funding agency in the public, commercial, or not-for-profit sectors.

Conflict of Interest

The authors declare that there is no conflict of interest regarding this manuscript.

References

1. Wang, Z. Q., Li, L., Zhang, Y., Li, H., & Zhang, J. (2022). Fabrication of Cocatalyst NiO-Modified BiVO4 Composites for Enhanced Photoelectrochemical Performances. Frontiers in Chemistry, 10, 864143.

2. Bai, Y., Zhao, X., Chen, H., & Li, J. (2025). BiVO4-based heterojunction photocatalysts for energy and environmental applications. Chemical Communications.

3. Zhang, Y., Liu, J., Chen, X., & Wang, H. (2025). Recent Progress in Bismuth Vanadate-Based Photocatalysts for Photocatalytic Degradation. Nanomaterials, 15(5), 331.

4. Nguyen, B. D., Tran, T. T., Pham, V. H., & Lee, J. (2025). Strategies for Enhancing BiVO4 Photoanodes for PEC Water Splitting: A State-of-the-Art Review. Nanomaterials, 15(19), 1494.

5. Navarrete-Cevallos, L. E., Vargas, R., & Espinoza-Montero, P. J. (2025). Fundamentals and environmental applications of bismuth vanadate through photoelectrocatalysis. npj Clean Water, 8, 96.

6. Heckel, S., Simmchen, J., & Ebbens, S. (2024). An Account on BiVO4 as Photocatalytic Active Matter. Accounts of Materials Research.

7. Tachikawa, T., Ochi, T., & Kobori, Y. (2016). Crystal-Face-Dependent Charge Dynamics on a BiVO4 Photocatalyst Revealed by Single-Particle Spectroelectrochemistry. ACS Catalysis, 6(4), 2250-2256.

8. Salih, A. K., Khan, A. Z., Drmosh, Q. A., Kandiel, T. A., Qamar, M., Jahangir, T. N., Ton-That, C., & Yamani, Z. H. (2024). Nanostructured BiVO4 Photoanodes Fabricated by Vanadium-Infused Interaction for Efficient Solar Water Splitting. ACS Applied Nano Materials.

9. Cheng, S., Zhang, Y., Li, X., & Chen, Z. (2025). Enhanced Photoelectrochemical Performance of BiVO4 Photoanodes through Surface Co-modification. Micromachines, 16(8), 866.

10. Wannakan, K., Khansamrit, K., Boonmak, J., & Phuruangrat, A. (2023). Ultrasound-Assisted Synthesis of a ZnO/BiVO4 S-Scheme Heterojunction Photocatalyst for Degradation of Reactive Red 141 Dye and Oxytetracycline Antibiotic. ACS Omega.

11. Sisay, E. J., Sen, T. K., & Ang, H. M. (2023). Application of BiVO4/TiO2/CNT Composite Photocatalysts for Membrane Fouling Control and Photocatalytic Membrane Regeneration during Dairy Wastewater Treatment. Catalysts, 13(2), 315.

12. Sisay, E. J., Sen, T. K., & Ang, H. M. (2022). Visible-light-driven photocatalytic PVDF-TiO2/CNT/BiVO4 hybrid nanocomposite ultrafiltration membrane for dairy wastewater treatment. Journal of Water Process Engineering.

13. Cai, P., Zhou, S., Ma, D., Liu, S., Chen, W., & Huang, S. (2015). Fe2O3-Modified Porous BiVO4 Nanoplates with Enhanced Photocatalytic Activity. Nano-Micro Letters, 7(2), 183-193.

14. Lecki, T., Zielinska-Jurek, A., & Hupka, J. (2024). Z-Scheme BiVO4/g-C3N4 Photocatalyst-With or Without Reduced Graphene Oxide? Molecules, 29(21), 5092.

15. Haryadinaru, G. H., Setyaningtyas, T., & Riapanitra, A. (2025). Nigella sativa-mediated synthesis of BiVO4/g-C3N4 composites for the removal of methylene blue dye. Bulletin of Chemical Reaction Engineering & Catalysis, 20(2), 346-358.

16. Riapanitra, A., Setyaningtyas, T., & Haryadinaru, G. H. (2025). Photodegradation of Methylene Blue Dye Using BiVO4/g-C3N4 Composites under Visible Light Irradiation. Jurnal Kimia Sains dan Aplikasi.

17. Trinh, D. T. T., Nguyen, T. T., Nguyen, V. H., & Vo, D. V. N. (2021). New insight into the photocatalytic degradation of organic pollutants using BiVO4/SiO2/GO nanocomposite. Environmental Science and Pollution Research.

18. Khan, N. A., Khan, A., Rahman, Z. U., & Ahmad, A. (2022). Efficient photodegradation of Orange II dye by nickel oxide nanoparticles and nanoclay supported nickel oxide nanocomposite. Applied Water Science, 12, 108.

19. Khairnar, S. D., & Shrivastava, V. S. (2019). Facile synthesis of nickel oxide nanoparticles for the degradation of methylene blue and rhodamine B dye: A comparative study. Journal of Taibah University for Science, 13(1), 1108-1118.

20. Shubha, J. P., Sowmya, H. V., Lakshmeesha, T. R., & Kumar, M. R. A. (2023). A green approach for the degradation of toxic textile dyes by nickel oxide nanoparticles: Photocatalytic and kinetic approach. Journal of King Saud University - Science, 35(5), 102696.

21. Barzinjy, A. A., Hamad, S. M., Aydin, S., Ahmed, M. H., & Hussain, F. H. S. (2020). Green and eco-friendly synthesis of nickel oxide nanoparticles and its photocatalytic activity for methyl orange degradation. Journal of Materials Science: Materials in Electronics.

22. Hariani, P. L., Said, M., Rachmat, A., Salni, Aprianti, N., & Amatullah, A. F. (2022). Synthesis of NiFe2O4/SiO2/NiO Magnetic and Application for the Photocatalytic Degradation of Methyl Orange Dye under UV Irradiation. Bulletin of Chemical Reaction Engineering & Catalysis, 17(4), 699-711.

23. Haq, S., Sarfraz, A., Menaa, F., Shahzad, N., Din, S. U., Almukhlifi, H. A., Alshareef, S. A., Al Essa, E. M., & Shahzad, M. I. (2022). Green Synthesis of NiO-SnO2 Nanocomposite and Effect of Calcination Temperature on Its Physicochemical Properties: Impact on the Photocatalytic Degradation of Methyl Orange. Molecules, 27(23), 8420.

24. Orimolade, B. O., Arotiba, O. A., & Mamba, B. B. (2020). Towards visible light driven photoelectrocatalysis for water treatment: Application of a FTO/BiVO4/Ag2S heterojunction anode for the removal of emerging pharmaceutical pollutants. Scientific Reports, 10, 5348.

25. Zhao, W., Tu, X., Wang, X., & Ni, S. (2019). Novel p-n heterojunction photocatalyst fabricated by flower-like BiVO4 and Ag2S nanoparticles: Simple synthesis and excellent photocatalytic performance. Chemical Engineering Journal, 361, 1292-1301.

26. Guan, B., Chen, J., Li, Z., Zhuang, Z., Chen, Y., Ma, Z., Guo, J., Zhu, C., Hu, X., Zhao, S., et al. (2024). Review on Synthesis, Modification, Morphology, and Combination of BiVO4-based Catalysts for Photochemistry: Status, Advances, and Perspectives. Energy & Fuels, 38(2), 806-853.

27. Kamble, G. S., Natarajan, T. S., Patil, S. S., Thomas, M., Chougale, R. K., Sanadi, P. D., Siddharth, U. S., & Ling, Y.-C. (2023). BiVO4 As a Sustainable and Emerging Photocatalyst: Synthesis Methodologies, Engineering Properties, and Its Volatile Organic Compounds Degradation Efficiency. Nanomaterials, 13(9), 1528.

28. Sindhu, M., Sharma, S., Somvanshi, A., Jasrotia, R., Gusain, M., George, N., Tabasum, S., Sharma, D., & Kumar, K. (2026). Strategic engineering of BiVO4 photocatalysts for efficient Solar-Driven systems: Advances, Limitations, and future prospects. Advanced Composites and Hybrid Materials.

29. Reyes-Vallejo, O., Cano, F. J., Sanchez-Albores, R., Luevano-Hipolito, E., Serrano-Ramirez, R. P., Hernandez-Cruz, M. C., Valencia, D., Torres-Martinez, L. M., & Velumani, S. (2025). Sustainable combustion synthesis of BiVO4 using orange peel for photocatalytic applications. Journal of Materials Science: Materials in Electronics, 36, 1251.

30. Minisha, S., Johnson, J., Mohammad, S., Gupta, J. K., Aftab, S., Alothman, A. A., & Lai, W.-C. (2024). Visible Light Photocatalytic Degradation of Environmental Pollutants Using Zn-Doped NiO Nanoparticles. Water, 16(2), 340.

31. Pavithra, M., Blair, N. J., & Jessie Raj, M. B. (2023). Zn-doped NiO nanocomposites for efficient solar light-assisted wastewater treatment and its profound for low phytotoxic and antibacterial applications. Plant Nano Biology, 6, 100054.

32. Gomaa, H. E., El-Maghrabi, H. H., Gomaa, F. A., Raynaud, P., & Nada, A. A. (2024). Enhanced Photodegradation of Acetaminophen Using Efficient ZnO-NiO Nanofibers. Catalysts, 14(7), 403.

33. Yasmeen, S., Burratti, L., Rugnini, L., Gismondi, A., de Lapuente, J., Puglia, D., Kenny, J. M., & Giovannetti, R. (2024). Photocatalytic Degradation of Organic Pollutants-Nile Blue, Methylene Blue, and Bentazon Herbicide-Using NiO-ZnO Nanocomposite. Nanomaterials, 14(5), 470.

34. Iqbal, N., Huang, X., Mohamedali Hamid, K., Yuan, H., Batool, I., & Yang, Y. (2025). Efficient Visible-Light-Driven Photocatalysis of BiVO4@Diatomite for Degradation of Methoxychlor. Catalysts, 15, 672.

35. Long, Z., et al. (2024). Construction of BiVO4/CoPc S-scheme heterojunctions with enhanced photothermal-assisted photocatalytic activity. Science China Materials, 67, 550-561.

36. Mohan, P., Mallapur, S., Prathibha, C. P., Rajesh, B. M., Ullah, I., Kandaiah, S., & Gopinathan, S. K. (2025). BiVO4/SnS2 S-scheme heterojunction for improved photocatalytic performance under visible light: charge carrier mechanism validation by DFT and electrochemical studies. Applied Physics A, 131, 967.

37. Chen, D., Hu, S., Jia, Z., Zhang, Y., Zhang, B., Liu, S., & Li, X. (2025). Construction of S-Scheme BiVO4/Bi2O2S Heterojunction for Highly Effective Photocatalysis of Antibiotic Pollutants. Molecules, 31(1), 136.

38. Le-Duy, N., et al. (2023). Pt/PtOx Nanoparticle-Decorated BiVO4 Pinelike Structure for Enhanced Sulfamethoxazole Mineralization under Visible Light Irradiation. ACS Applied Nano Materials.

39. Fu, W., Lu, G., Wang, X., Xie, X., & Sun, J. (2024). Construction of BiVO4@NiCo2O3 Heterojunction to Promote Photocatalytic CO2 Reduction. ChemPhotoChem, 8(11).

40. Wan, X., et al. (2023). Enhanced Photoelectrochemical Water Oxidation on BiVO4 Photoanodes Functionalized by Bimetallic Dicyanamide Molecular Catalysts. Sustainability, 15(4), 3129.